CI&CEQ

Available on line at
Association of the Chemical Engineers AChE
www.ache.org.rs/CICEQ
Chemical Industry & Chemical Engineering Quarterly 15 (3) 137–142 (2009) CI&CEQ

ALEKSANDAR KOJOVIĆ[1]
IRENA ŽIVKOVIĆ[2]

[1]*University of Belgrade, Faculty of Technology and Metallurgy, Karnegijeva 4, 11000 Belgrade, Serbia*
[2]*Institute of Security, Kraljice Ane bb, 11000 Belgrade, Serbia*

SCIENTIFIC PAPER

**UDC 678.7/.742**

**DOI: 10.2298/CICEQ0903137K**

# DAMAGE DETECTION OF HYBRID ARAMID/ /METAL-PVB COMPOSITE MATERIALS USING OPTICAL FIBER SENSORS

*Embedding optical fiber sensors within laminar thermoplastic composite material results in forming a system known as «smart structure». These sensors present the information about the inner structure health during the material exploitation and especially in the case of exterior impacts when a geometric configuration or the property changes of the material should be expected. This paper evaluates the feasibility of the real-time monitoring of indentation and low energy impact damage in composite laminates from indentation loading and Charpy pendulum impact, using the embedded intensity-based optical fiber sensors. An optical fiber sensing system, which relies solely on monitoring light intensity for providing the indication of the composite structural health, offers simplicity in design and cost-effectiveness. For this, aramid/polyvinylbutyral (PVB) and aramid/metal/PVB laminates with embedded optical fibers were fabricated. Four configurations of woven composites were tested, namely, aramid/PVB, and aramid/metal/PVB in three stacking sequences of aramid and metallic woven layers. The initiation of damage and fracture during testing was detected by observation of the intensity drop of light signal transmitted through an optical fiber.*

*Key words: thermoplastic composites; optical fiber sensors; indentation damage detection; low energy impact damage detection; real-time health monitoring.*

In addition to classical methods for damage detection in composite materials with polymer matrix (ultrasound [1], acoustic emission [2,3]), optical fiber sensors (OFS) are widely used to monitor and precisely estimate the material behavior during its manufacturing and exploitation life. Different OFS configuration can be found which mostly depends on an optical fiber type being used and their light sensitivity. Numerous investigations on Smart Materials with embedded interferometric OFS such as Fabry-Perot [4-6], Michelson [7], and Bragg grating sensors [8-12] were made.

The shape and structure of intensity based optical fiber sensors allow their simple embedding in the host material without disturbing its basic mechanical properties, and therefore, they can be used as reliable, long-term automated sensors for real time structure damage and deformation detection [13,14]. Many authors noticed delamination within composite structures by using intensity based OFS [15-18] and studied damage detection caused by low energy impact [19,20]. Hofer [21] has embedded a net of uncoated OFS of different diameters into the GFRP and CFRP. The purpose of his investigation was a possibility of exploitation of such a smart material as a component in Airbus production line. During his study, he managed to develop the system for automated indication of the damage that is invisible by bare eye but detectable from the pilot cabin in real time. This system has opened a possibility for the routine control minimizetion or even its abrogation.

Most of investigated composites contain thermoreactive polymer as a matrix. Živković *et al.* [22,23] conducted the investigation on thermoplastic composite material aramid fiber/poly(vinylbutyral). This work has shown that this specific material has the energy absorption capacity 5.5 times higher than the capacity of traditionally used materials with the same reinforcement. Kojović *et al.* [24] conducted the experimental low energy impact testing of this laminar composite material with embedded OFS in order to ob-

Corresponding author: A. Kojović, University of Belgrade, Faculty of Technology and Metallurgy, Karnegijeva 4, 11000 Belgrade, Serbia.
E-mail: koja@tmf.bg.ac.rs
Paper received: 29 January, 2009.
Paper revised: 20 May, 2009.
Paper accepted: 30 May, 2009.

serve and analyze the response of the material under multiple low-energy impacts. The obtained signals were analyzed to find the appropriate method for real time damage monitoring.

In this work, the intensity based OFS were embedded in referred material and, so made, smart material was tested by indentation loading and Charpy pendulum impact. The results were compared and the corresponding analyses were conducted.

## EXPERIMENTAL

### Properties of reinforcement

Two types of reinforcement were used, woven aramid fabric and metal woven wire. Properties of aramid fabric Kevlar 129, superficial mass of 280 g/m$^2$ are listed in Table 1.

*Table 1. Properties of aramid fibers*

| Density, g/cm$^3$ | 1.44 |
|---|---|
| Ultimate tensile strength, cN/tex | 235 |
| Tensile strength, MPa | 3380 |
| Elongation at break point, % | 3.4 |
| Moisture content, % | 7 |
| Decomposition temperature, °C | 560 |
| Sound velocity, m/s | 8660 |

Properties of metal woven wire* are listed in Table 2.

*Table 2. Properties of metal woven wire*

| Mesh | 250 |
|---|---|
| Diameter, mm | 0.040 |
| Free surface, % | 38 |
| Mesh opening, μm | 63 |
| Amount, kg m$^2$ | 0.20 |
| Steel type | Stainless steel AISI 304/316 |

### Matrix properties

Thin poly(vinylbutyral) (PVB) foils were used as a matrix in the composite material. The properties of thermoplastic PVB** are listed in Table 3.

*Table 3. Thermoplastic matrix properties*

| Density, g/cm$^3$ | 1.058 |
|---|---|
| Refractive index | 1.48 |
| Tensile strength, MPa | 23 |
| Elongation at break, % | 210 |
| Tensile modulus, MPa | 5 |
| Poisson's ratio | ±0.5 |
| Shore "A" Hardness | 64 |
| Specific heat, J/kg K | 2100 |
| Glass transition temperature, °C | 16 |
| Thermal conductivity, W/m K | 0.21 |
| Dielectric constant at 1 kHz | 4 |
| Dissipation factor at 1 kHz | $1.8\times10^{-4}$ |

### Optical fiber sensors properties

Multimode optical fibers*** were used as sensors. Properties are listed in Table 4.

*Table 4. Properties of optical fiber*

| Wavelength range, nm | 850-1300 |
|---|---|
| Signal intensity drop, dB/km | 2.87-3.66 |
| Bandwidth, MHz/km | 522-748 |
| NA | 0.27 |
| Diameter of core, cladding and coating, μm | 62.5/125/250 |
| Coating | A |
| Type of fiber | H2E103EB |

### Shaping process and properties of composite material

A uniform alternating packing of 25 reinforcement layers and 24 matrix layers combines the chosen materials alternately. Laminates were hot-pressed inside closed mold coated with silicon oil. Afterwards, specimens were left in a mold under slightly increased working pressure to cool from maximal working temperature of 180 to 100 °C, and then were taken out of mold to cool at room temperature under load of 10 kg [22]. Samples OH1 and OH4 were made with metal mesh as reinforcement in every third layer, while other reinforcement layers were aramid fabric. Sample OH2 was made with metal mesh as reinforcement in even layers, and aramid fabric in odd layers. Sample OH3 was made with aramid fabric as reinforcement in every third layer, while other reinforcement layers were metal mesh. Samples K1 and A1 were made only with aramid fabric as reinforcement. At the end, total masses of samples were measured and the mass percentage of sample's specific components was calculated. The results are listed in Table 5.

Optical fiber sensors were embedded into the last layer of composite material according to the procedure described in earlier work [25].

In Fig. 1 the sample of the composite material with embedded optical fibers used for indentation load testing is shown. The damage caused by the indenter

*Original properties given by manufacturer (Spörl GmbH).

**Original properties given by manufacturer - Saflex® (Monsanto Company's registered trade-mark for poly(vinylbutyral)).

***Original properties given by manufacturer (Iskra Opto-elektronika).

*TABLE 5. Samples total mass, mass % of specific components*

| Description | Sample | | | | | |
|---|---|---|---|---|---|---|
| | A1 | K1 | OH1 | OH2 | OH3 | OH4 |
| Total specimen mass, g | 215.8 | 230.0 | 206.3 | 206.3 | 206.9 | 207.6 |
| Metal wire in specimen total mass, mass% | 0 | 0 | 16.0 | 25.7 | 33.8 | 16.2 |
| Reinforcement, mass% | 66.2 | 65.2 | 52.3 | 35.2 | 21.7 | 48.3 |
| Metal wire in reinforcement total mass, mass% | 0 | 0 | 23.4 | 42.2 | 39.5 | 25.1 |
| Aramid fibers in reinforcement total mass, mass% | 100 | 100 | 76.6 | 57.8 | 60.5 | 74.9 |
| Matrix, mass% | 33.8 | 34.8 | 31.7 | 39.1 | 44.5 | 35.5 |

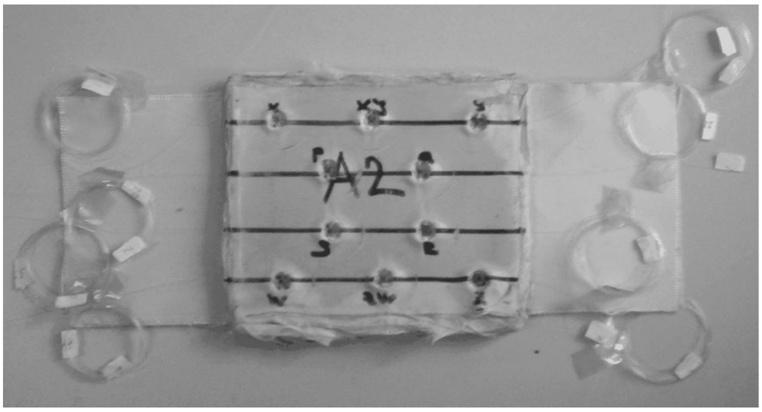

*Figure 1. Sample of composite material after indentation.*

could clearly be seen, because the pictures were taken after the experiment. Optical fiber sensors were undamaged after the experiment.

For low energy impact testing, each sample was divided into multiple specimens. Figure 2 shows a pattern of specimens for sample OH2. Other samples (K1 and OH4) were divided in the same way. The photo of specimen with an embedded optical fiber is shown in Fig. 3.

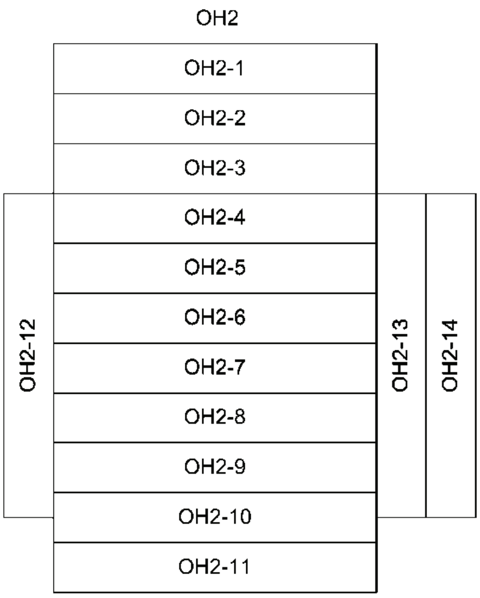


*Figure 2. Pattern of specimens in sample OH2.*

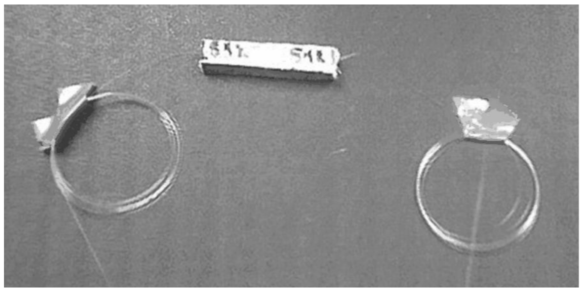

*Figure 3. Specimen with embedded optical fiber.*

### Measuring equipment

Manufactured composite specimens with optical fibers were subjected to static loading by the adapted tensile testing machine. Loading was directed so the optical fibers were on the farthest position from the indentation loading point. The opto-electronic part of the measurement system consists of four (some of the measurements were made with three) light emitting diodes (LEDs) as the light source for optical fibers, and four (three) photo-detectors for the light intensity measurement (shown in Fig. 4). The output signal voltage acquisition from the photo detectors device was conducted using AD converter card and a personal computer.

In this work, only indentations which were made directly above the optical fiber are considered, because the sensor has maximum sensitivity in this position.

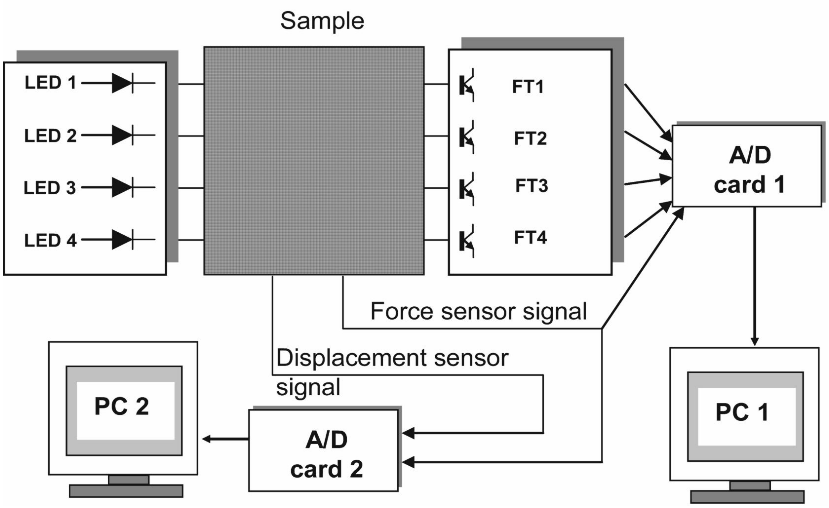


*Figure 4. Measurement equipment for indentation loading.*

For low energy impact measurements the light from the LED (peak wavelength 840 nm) was launched to the embedded optical fiber and was propagated to the phototransistor based photo detector (Fig. 5). The output signal from the photo detector was connected to the data acquisition system based on AD card and the personal computer. The source for low energy impacts was Charpy's pendulum, as described in previous work [24]. Sampling time was 40 μs with the acquisition time of 80 ms after the impact and 4 ms before the impact.

## RESULTS AND DISCUSSION

Figures 6a, 6c and 6e show OFS signal intensity drop during indentation loading, while Figs. 6b, 6d and 6f show OFS signal during Charpy's pendulum impact. Figures 6a-6f could be compared in both, vertical and horizontal direction.

As pressure is applied on OFS, the amount of light which passes through it drops. The pressure rises throughout indentation or low energy impact, so a temporary rise in OFS signal could only be explained as a development of damage which temporarily releases the pressure from OFS. In Figs. 6a, 6c and 6e it could be seen that with lowering the amount of Kevlar in composite the first appearance of damage in material occurs earlier (in sense of signal level, time is irrelevant here because the speed and beginning of indentation was not the same) during the signal drop. In Fig. 6a, the damage occurs near the end of indentation, in Fig. 6c it occurs at about 2/3 of indentation, and in Fig. 6e it is slightly after half of indentation, which corresponds to toughness decrease of the composite material (metal mesh has lower toughness than aramid fabric). The same could be seen during the low energy impact, in Figs. 6b, 6d and 6f.

Comparing Figs. 6a-6d, an analogy between the indentation load signal and a drop zone in low energy impact signal could be seen. Figures 6e and 6f could

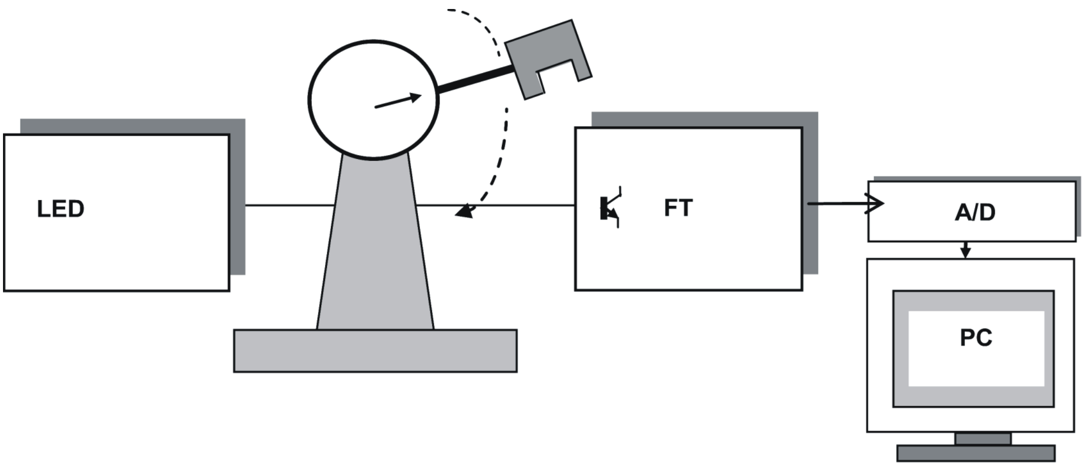


*Figure 5. Measurement equipment for low energy impact.*

not be directly compared because different ratio of material reinforcement was used, but as the differrence in mass percent of metal wire is less then 3%, the similarity of signals could also be seen.

In Fig 7, it could be seen that at the same moment when the damage in material occurs the indentation force load drops and the gradient of loading is changed (first three occurrences are marked as I, II

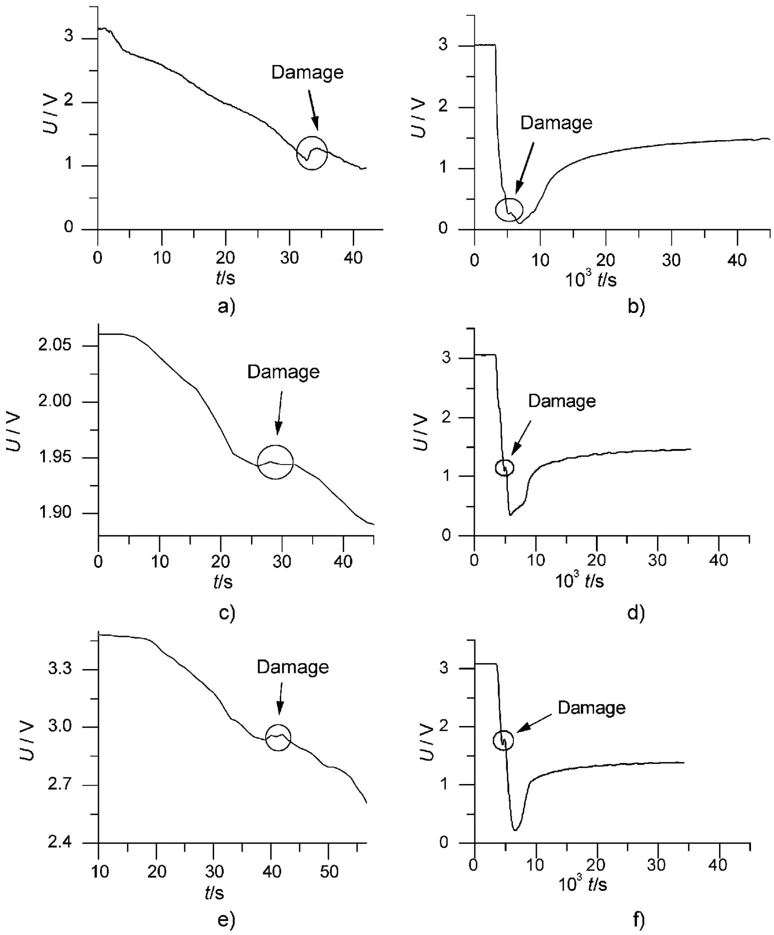


*Figure 6. a) Indentation loading, specimen A1 point R, b) signal on specimen K1-5 during first low energy impact, c) indentation loading, specimen OH1, point 6, d) signal on specimen OH4-7 during first low energy impact, e) indentation loading, specimen OH3, point 6, f) signal on specimen OH2-3 during the first low energy impact.*

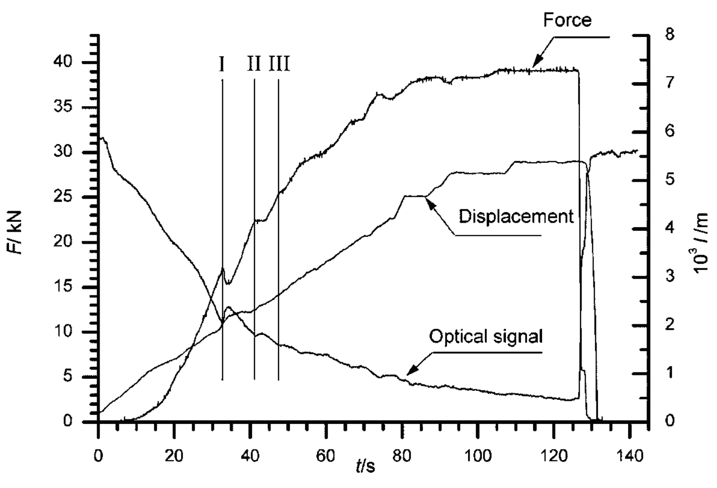


*Figure 7. Signals measured during the indentation test on specimen A1, point R.*

and III). The explanation of this phenomenon can be the fact that indentation, after piercing through the first layer of the composite plate, ran into the layer of thermoplastic matrix. This is a medium of lower strength than composite and therefore an area of lesser local stress around the optical fiber. Signal intensity increases until the point when the indentator touches the second layer of the composite material, renewing stress around the fiber and decreasing the signal intensity as a consequence. This sequence repeats with following layers as force increase. After unloading, the signal intensity restores its initial value, which indicates an undamaged structure of optical fibers during tests.

## CONCLUSIONS

The results show that the intensity based optical fibers could be used for measuring the damage in laminar thermoplastic composite materials and as a reliable automatic system for a long-term structure health monitoring. OFS are useful for static loading (indentation) as well as for low energy impact damage monitoring. Light signal intensity drops in an optical fiber in response to applied loading on composite material. The acquired optical fiber signals depend on the type of material, but the same set of rules for damage detection (relatively different, depending on type of the material) could be specified. There is an analogy in behaviour of material with the same composition in both types of applied loading (indentation and low energy impact). The appearance of damage in material, as it could be seen in OFS signals, is in correspondence with material toughness and strength.

## REFERENCES

[1] C. Potel, T. Chotard, J. F. Belleval, M. Benzeggagh, Composites B **29**B (1998) 159-169

[2] W. Haselbach, B. Lauke, Compos. Sci. Tech. **63** (2003) 2155-2162

[3] D. Sung, C. Kim, C. Hong, Composites B **33** (2002) 35-43

[4] A. E. Bogdanovich, D. E. Wigent III, T. J. Whitney, SAMPE J. **39** (2003) 6-15

[5] A. Kalamkarov, S. Fitzgerald, D. MacDonald, A. Georgiades, Compos. Sci. Technol. **60** (2000) 1161-1169

[6] A. Malki, R. Gafsi, L. Michel, M. Labarrere, P. Lecoy, Appl. Opt. **35** (1998) 5198-5201

[7] I. B. Kwon, C. G. Kim, C. S. Hong, Compos. Sci. Technol. **57** (1997) 1639-1651

[8] K. S. C. Kuang, R. Kenny, M. P. Whelan, W. J. Cantwell, P. R. Chalker, Compos. Sci. Techol. **61** (2001) 1379-1387

[9] R. Jones, S. Galea, Compos. Struct. **58** (2002) 397-403

[10] M. Studer, K. Peters, J. Botsis, Composites B **34** (2003) 347-359

[11] S. Takeda, Y. Okabe, N. Takeda, Composites A **33** (2002) 971-980

[12] J. Park, S. Lee, O. Kwon, H. Choi, J. Lee, Composites A **34** (2003) 203-216

[13] R. Hadžić, S. John, I. Herszberg, Compos. Struct. **47** (1999) 759-765

[14] D. C. Seo, J. J. Lee, Compos. Struct. **32** (1995) 51-58

[15] L. Rippert, M. Wevers, S. Huffel, Compos. Sci. Technol. **60** (2000) 2713-2724

[16] P. S. Uskoković, I. Balac, Lj. Brajović, M. Simić, S. Putić, R. Aleksić, Adv. Eng. Mater. **3** (2001) 492-496

[17] N. Takeda, Int. J. Fatigue **24** (2002) 281-289

[18] R. M. Measures, D. W. Glossop, J. Lymer, M. Leblanc, J. West, S. Dubois, W. Tsaw, R. C. Tennyson, Appl. Opt. **28** (1989) 2626-2633

[19] K. S. C. Kuang, W. J. Cantwell, J. Mater. Sci. Lett. **21** (2002) 1351-1354

[20] P. S. Uskoković, Lj. Brajović, M. Simić, S. S. Putić, R. Aleksić, Adv. Compos. Mater. **9** (2000) 175-185

[21] B. Hofer, Composites **18** (1987) 309-316

[22] I. Živković, P. Perišic, Z. Burzić, P. Uskoković, R. Aleksić, Proc. of 23$^{rd}$ SAMPE Eur. Int. Conf., Paris, 2002, pp. 249--260

[23] I. D. Živković, P. I. Perisić, Z. H. Burzić, P. S. Uskoković, R. R. Aleksić, J. Adv. Mater. **37** (2005) 23-31

[24] A. Kojović, I. Živković, Lj. Brajović, D. Mitraković, R. Aleksić, Mater. Sci. Forum **494** (2005) 481-486

[25] I. Živković, Lj. Brajović, P. Uskoković, R. Aleksić, J. Adv. Mater. **37** (2005) 33-37.